Effect of annealing and Nd concentration on the photoluminescence of Nd 3 + ions coupled with silicon nanoparticles

O. Debieu, D. Bréard, A. Podhorodecki, G. Zatryb, J. Misiewicz, C. Labbé, J. Cardin, and F. Gourbilleau

Citation: Journal of Applied Physics **108**, 113114 (2010); doi: 10.1063/1.3510521
View online: http://dx.doi.org/10.1063/1.3510521
View Table of Contents: http://scitation.aip.org/content/aip/journal/jap/108/11?ver=pdfcov
Published by the AIP Publishing

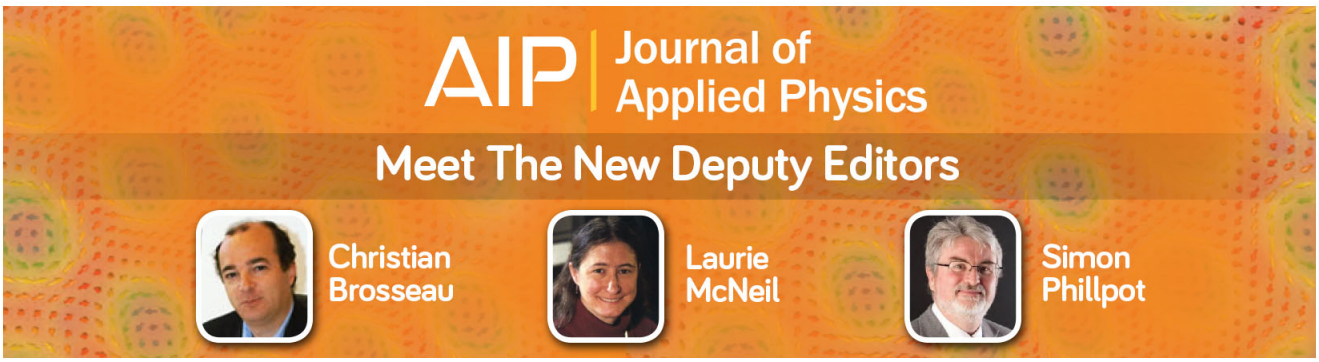

Effect of annealing and Nd concentration on the photoluminescence of Nd^{3+} ions coupled with silicon nanoparticles

O. Debieu,[1,a)] D. Bréard,[1] A. Podhorodecki,[2] G. Zatryb,[2] J. Misiewicz,[2] C. Labbé,[1] J. Cardin,[1] and F. Gourbilleau[1]
[1]*CIMAP, UMR CNRS/CEA/ENSICAEN/UCBN, Ensicaen 6 Bd Maréchal Juin, 14050 Caen Cedex 4, France*
[2]*Institute of Physics, Wroclaw University of Technology, Wybrzeze Wyspianskiego 27, 50-370 Wroclaw, Poland*

(Received 2 September 2010; accepted 30 September 2010; published online 9 December 2010)

We report on the microstructure and photoluminescence (PL) properties of Nd-doped SiO_2 thin films containing silicon nanoparticles (Si-np) as a function of the annealing temperature and the Nd concentration. The thin films, which were grown on Si substrates by reactive magnetron co-sputtering, contain the same Si excess. Fourier transform infrared (FTIR) spectra show that a phase separation occurs during the annealing due to the agglomeration of the Si excess resulting in the formation of Si-np. Besides, after annealing, the films exhibit PL from excitonic states confined in Si-np. We showed that the intensity of the PL of Nd^{3+} ions that occurs at ~0.92, 1.06, and 1.4 μm is maximal at low Nd concentration and while well-passivated Si-np are formed. FTIR and x-ray measurements showed that the increase in the Nd incorporation has detrimental effects on the PL of Nd^{3+} because of the formation of Nd_2O_3 nanocrystals and inherent disorder in the SiO_2 host matrix. PL excitation measurements demonstrate that the PL of Nd^{3+} ions is nonresonant and follows the excitation of Si-np giving new evidence of the energy transfer from Si-np toward the rare earth ions. © *2010 American Institute of Physics*. [doi:10.1063/1.3510521]

I. INTRODUCTION

Rare earth (RE) ions, especially Er^{3+} and Nd^{3+} ions, have attracted a considerable interest these last years because of their industrial applications. The former has been used for telecommunications because of the interesting radiative $^4I_{13/2} \rightarrow {}^4I_{15/2}$ transition at 1.54 μm that corresponds to the absorption minimum of standard silica optical fibers.[1] The latter has been highly used for solid-state laser applications due to the $^4F_{3/2} \rightarrow {}^4I_{11/2}$ transition at 1.06 μm which presents a high stimulated emission cross-section ($\approx 3 \times 10^{-19}$ cm^2).[2] Furthermore, this transition occurs in a four-level medium where the lower level is well above the ground state which contrasts with the 1.54 μm transition of Er that ends on the ground state in a three-level system. As a result, the achievement of population inversion of Nd^{3+} ions can be achieved with a lower threshold, thereby offering high laser gain efficiency like in the case of Nd:YAG crystal that is the most notable success of RE-based laser. One of the challenging fields of the last decades concerns silicon compatible light sources and amplifiers which are getting more and more attractive since they can be integrated to microelectronics devices.[3] Unfortunately, whatever the host matrix, RE ions suffer from a low absorption cross-section as it has been reported in the case of Er^{3+} ions[4,5] and Nd^{3+} ions.[2,6,7] Since the discovery of the sensitizing effect of Si-nanoparticles (Si-np) toward RE emission,[8] RE-doped nanostructured Si-based films are promising for the achievement of future devices optically excited. Kenyon *et al.*[9] demonstrated that the presence of Si-np in a SiO_2 host matrix resulted to an increase in the Er^{3+} photoluminescence (PL) by a factor of 100 and an enhancement of the effective absorption cross section by four orders of magnitude.[9,10] In such systems, RE ions benefit from the high absorption cross-section of Si-np by energy transfer. In contrast to Er^{3+} ions, such materials doped with Nd, have not been widely investigated and, accordingly, the energy transfer between Si-np and Nd^{3+} ions.[11–18] Several authors have demonstrated that the energy transfer is more effective with small Si-np. Watanabe *et al.*[11] have shown that the increase in the Si-np average size from 2.7 to 3.8 nm results in a decrease in the PL intensity of Nd^{3+} ions. In the same way, Seo *et al.*[12] have observed a decrease in the PL intensity of Nd^{3+} ions at 1.06 μm with the increase in the excess of Si, i.e., the increase in the Si-np average size. They concluded that only small Si-np which present excitonic states with a sufficient energy band-gap can excite the $^4F_{3/2}$ level of Nd^{3+} ions. The effect of the Nd concentration in the optical properties of Nd-doped Si-np/SiO_2 has been studied by several groups.[13,14] MacDonald *et al.*[13] have changed the Nd content from 0.19 to 1.29 at.%. They have obtained a maximum of the PL intensity for a Nd concentration of ~0.29 at.%. Such a result underlines the problem of concentration quenching of RE ions in such Si-np/SiO_2 systems whose mechanism remains unknown.

In this paper, we describe the microstructure of Nd-doped silicon rich silicon oxide (SRSO) thin layers synthesized by reactive magnetron sputtering by mean of Fourier transform infrared (FTIR) spectroscopy, and x-ray diffraction (XRD). Their optical properties were investigated through PL, and total PL excitation measurements (TPLE). We examine the influence of the evolution of the microstructure as a function of the annealing temperature and the Nd content on the PL properties of the films. We could describe the proper

a)Electronic mail: olivier.debieu@ensicaen.fr.

conditions to obtain efficient PL of Nd^{3+} but also its limitations. The excitation energy dependence of Nd^{3+} is compared to the one of Si-np.

II. EXPERIMENT

In this work, amorphous hydrogenated Nd-doped SRSO thin films were deposited on p-type Si wafers by a reactive magnetron RF co-sputtering method that consists in sputtering simultaneously a pure SiO_2 target topped with Nd_2O_3 chips. The Nd concentration is monitored by the surface ratio between the Nd_2O_3 chips and the SiO_2 target. The sputtering gas is a mixture of argon and hydrogen; the latter enables to control the Si content of the deposited layers by reacting with oxide species in the plasma originating from the sputtering of the target. More details on the reactive sputtering method can be found elsewhere.[18] The films were grown at room temperature on Si substrates with a power density of 0.76 W/cm^2. The samples were subsequently annealed at high temperature ranging from 900 to 1100 °C in a dry nitrogen flow.

The infrared absorption properties were investigated by means of a Nicolet Nexus FTIR spectrometer at Brewster's incidence. The XRD measurements were performed using a Philips Xpert NPD Pro diffractometer mounted with a point scintillation detector in the θ-2θ configuration. The composition of the deposited layers was determined by Rutherford backscattering spectrometry while the refractive index (given at 1.95 eV), as well as the film thickness, were determined trough ellipsometric spectroscopy analyses.

The PL measurements were performed at room temperature using either a 266 nm semiconductor laser (3 W/cm^2) or an argon ion laser operating at 488 nm (7.6 W/cm^2) as excitation source. After 266 nm excitation, the UV-visible spectral range of the PL was detected by an HR4000 Ocean Optics spectrophotometer, while the near IR emission was collected by an InGaAs charge-coupled device camera after dispersion through a Jobin-Yvon TRIAX 550 monochromator. After 488 nm excitation, the PL was measured through a Jobin-Yvon THR 1000 monochromator mounted with a cooled Ge detector and a lock-in amplifier to record the near infrared spectra up to 1.5 μm. The visible spectra were recorded with a fast photomultiplier (Hamamatsu) after dispersion of the PL with a Jobin-Yvon TRIAX 180 monochromator. The 266 and 488 nm excitation wavelengths are nonresonant lines with Nd^{3+} ions so that only an indirect excitation of Nd trough the Si-np can occur.[6,14,16]

TPLE measurements were performed using a 450 W xenon arc lamp as the excitation source, which was connected to a 0.18 m Jobin Yvon monochromator. The excitation power density was about 0.1 W/cm^2 in the 210–480 nm excitation range. A beam splitter redirected a part of the excitation light to a power-meter in order to monitor the wavelength dependence of the Xe lamp power. Thus, each obtained PL spectrum was corrected by the excitation power. The PL spectra were measured with the Ocean Optics HR4000 spectrometer.

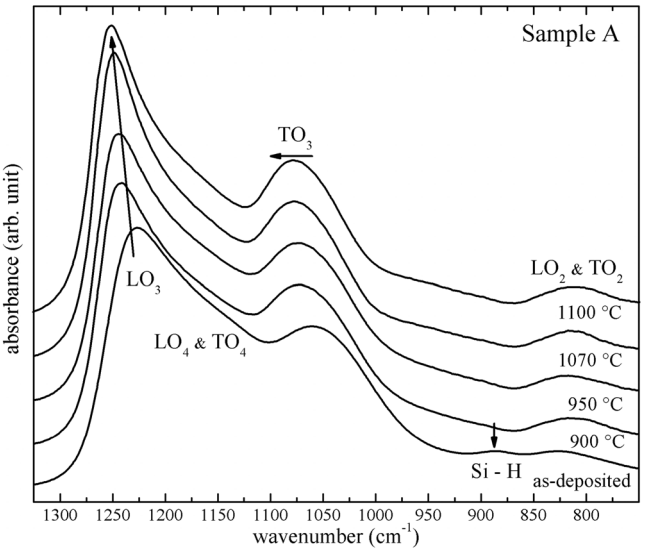

FIG. 1. Evolution of the FTIR spectra of sample A as a function of the annealing temperature. The spectra were normalized with respect to the TO_3 band intensity.

III. RESULTS

In this study, we were interested in four Nd-doped SRSO thin films which have the same Si excess fixed to ~7 at.%. After annealing at high temperature, Si-np are formed in the films in which the Nd content varied from 0.08 at.%, 0.27 at.%, 1.68 at.%, to 4.9 at.% (denoted as samples A, B, C, and D, respectively).

A. Microstructure

Figure 1 shows the evolution of the FTIR spectra of sample A as a function of the annealing temperature. The as-deposited sample shows a weak absorption band centered at ~880 cm^{-1} assigned to Si–H bonds. This band manifestly disappears after annealing because of the well known hydrogen desorption process. Several bands characteristics of amorphous SiO_2 are observed. The two prominent bands at 1220–1250 cm^{-1} and 1050–1070 cm^{-1} are assigned to longitudinal optical (LO_3) and transverse optical (TO_3) phonons of Si–O bonds, respectively. The TO_2, LO_2, LO_4, and TO_4 vibration modes are also present at 810 cm^{-1}, 820 cm^{-1}, 1160 cm^{-1}, and 1200 cm^{-1}, respectively. The attenuation of the TO_4–LO_4 pair modes with the annealing temperature indicates a reduction in disorder.[19] Besides, one can observe a progressive shift to higher wavenumbers of the TO_3 and LO_3 bands toward the stoichiometric positions of amorphous SiO_2 at 1076 cm^{-1} and 1256 cm^{-1}, respectively, while the annealing temperature was increased. It is explained by the condensation and agglomeration of the Si excess resulting in the formation of Si-np.[20,21] In the same time, the increase in the LO_3 bands intensity is related to the increase in the number of Si–O–Si bonds at the SiO_x/Si-np interface,[19,21] i.e., the increase in the density of Si-np.[22]

Figure 2 shows the evolution of the FTIR spectra of the samples annealed at 1100 °C as a function of the Nd concentration. One can observe that the LO_3 band intensity, which is constant at low Nd concentrations of 0.08 and 0.27

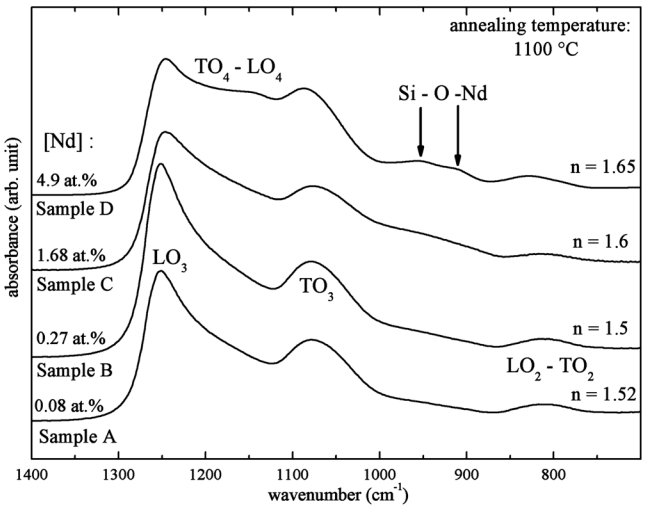

FIG. 2. Evolution of the FTIR spectra and the refractive indexes as a function of the Nd concentration.

at.%, significantly decreases while the Nd content was increased from 1.68 to 4.9 at.%. This evolution contrasts with the one of the TO_4–LO_4 pair modes. Indeed, the TO_4–LO_4 intensity remains constant a low Nd concentrations of 0.08 and 0.27 at.%, then, it progressively increases with increasing the Nd content. This shows that the incorporation of Nd generates disorder in the host SiO_2 matrix.

In the spectral range of 870 to 1000 cm^{-1}, on can observe a shoulder in the FTIR spectra of the low Nd-doped samples (A and B) which can originate from Si–O^- and Si–OH phonons.[23,24] However, one can exclude the existence of the Si–OH vibration mode after annealing at 1100 °C because of the hydrogen desorption. However, the emergence of two new weak absorption peaks centered at 910 and 950 cm^{-1} in the highest Nd-doped sample (sample D) suggests that other phonons are also optically active in this spectral range. These vibration peaks, which are exclusively distinguishable above an annealing temperature of 1100 °C, are attributed to asymmetric mode of Si–O–Nd bonds.[25] They strikingly coincide with the ones observed by several groups in neodymia-silica composites, which, interestingly, contained Nd_2O_3 nanocrystals.[28,29] The refractive indexes of each sample annealed at 1100 °C are shown in Fig. 2. Again, one can observe that the refractive index is rather constant at low Nd concentrations, and significantly increases while the Nd content was increased from 1.68 to 4.9 at.%. The increase in the volume fraction of a Nd_2O_3 phase, which has a refractive index of about 2 would also explain such behavior.[26]

In Fig. 3 is depicted the XRD spectra of sample A and D. In sample A, one band corresponding to amorphous SiO_2 is observed, while the pattern of sample D indicates the presence of additional phases. In the 27°–32° range, sample D shows various sharp peaks that are located above a band centered at ~29°. This band, and the 47.5° band, indicate the presence of nanocrystalline Si,[22,27] while the sharp and intense peaks located at 27.6°, 28.8°, and 30.7° are assigned to Nd_2O_3 crystals. However, the 28.8° peak may result from both crystalline Si and Nd_2O_3, for the sake of completeness. It is interesting to note that the 27.6° and 30.7° peaks fairly

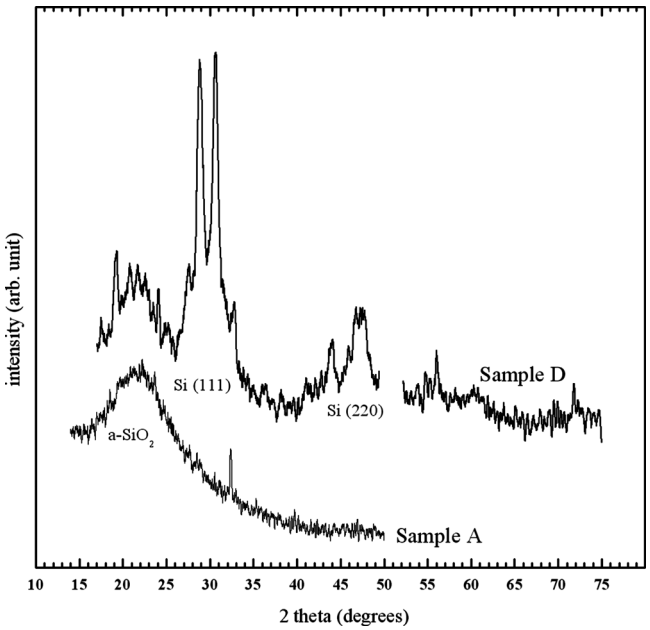

FIG. 3. XRD patterns of samples A and D after annealing at 1100 °C.

concur with the ones observed in neodymia-silica composites containing Nd_2O_3 nanocrystals by several researchers.[28,29] As a consequence, the presence of Nd_2O_3 and Si nanocrystals in sample D is clearly established, while such phases are not detected in sample A.

B. PL spectroscopy

Figure 4 shows the evolution of the room temperature PL spectra of sample A as a function of the annealing temperature. In the visible domain, sample A shows a broad PL band centered at about 740 nm after annealing. This PL band is originating from quantum-confined excitonic states in Si-np. The enhancement of the PL intensity of this PL band with the annealing temperature is characteristic for Si-np embedded in SiO_2. It is due to the increase in the Si-np density, as

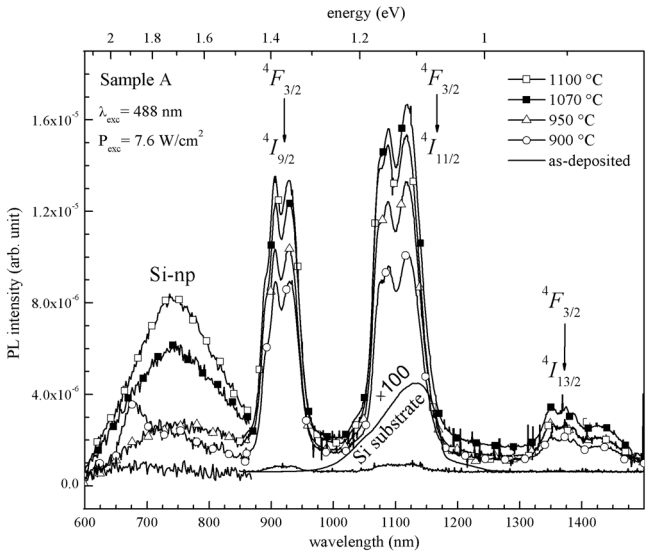

FIG. 4. Evolution of the PL spectra of sample A as a function of the annealing temperature.

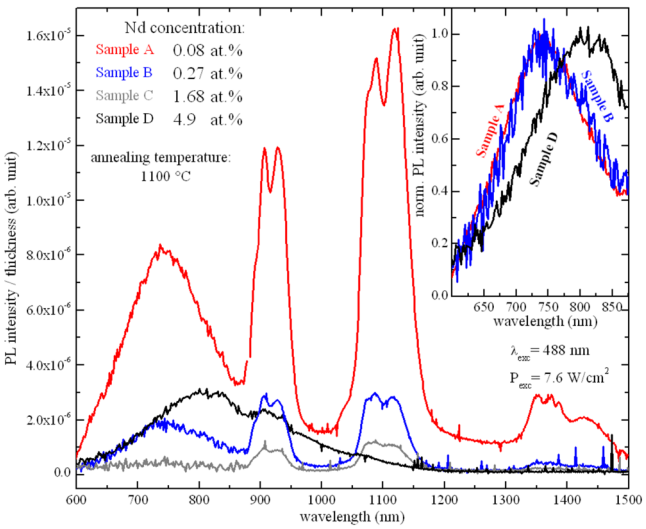

FIG. 5. (Color online) Evolution of the PL spectra as a function of the Nd concentration.

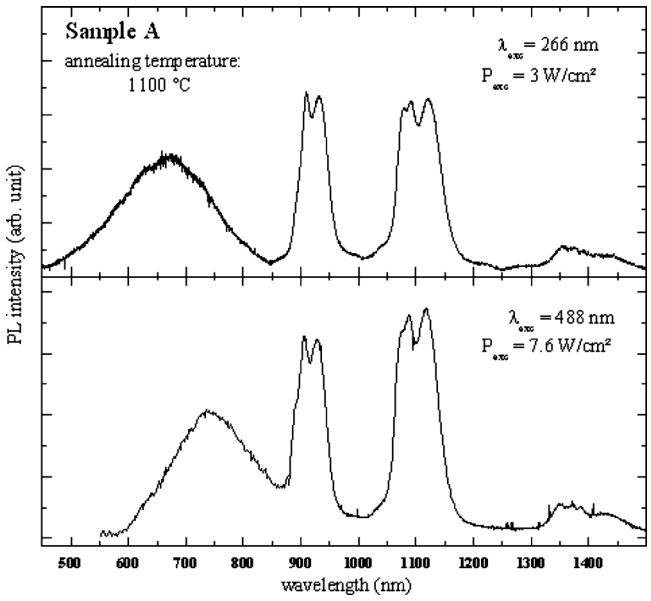

FIG. 6. PL spectra of sample A measured under the 266 and 488 nm excitation wavelengths.

showed by the increase in the LO_3 band intensity in the FTIR spectra (see Fig. 1),[22] and the improvement of their passivation,[30] as well as the decrease in disorder in the host matrix which provides sources of nonradiative recombination channels, as demonstrated by the decrease in the TO_4-LO_4 pair modes intensity in the FTIR spectra (see Fig. 1). Besides, it is generally admitted that 1100 °C is the optimal annealing temperature for the PL of Si-np. In the infrared domain, one can distinguish three peaks centered at around 920, 1100, and 1350 nm which correspond to the infra-4*f* shell transitions of Nd^{3+} ions from the $^4F_{3/2}$ level to the $^4I_{9/2}$, $^4I_{11/2}$, and $^4I_{13/2}$ levels, respectively. The presence of the PL of Nd^{3+} ions after nonresonant excitation brings to light the sensitizing effect of Si-np toward Nd^{3+} ions.

The Si substrate shows a weak room temperature broad PL band centered at 1130 nm. This band is intrinsic to crystalline doped-material and is originating from donor or acceptor species. Several authors demonstrated that the PL intensity of this band can nonmonotonously vary with the annealing temperature, and furthermore with the doping concentration.[31,32] Moreover, in our systems, the influence on the deposited layers on the Si substrate properties, in particular at the interface, is still unknown. As a consequence, in order to avoid any mistakes on the evaluation of the PL intensity of Nd^{3+} ions, we should not take the $^4F_{3/2} \rightarrow {}^4I_{11/2}$ transition into account since its position coincides with the one of the defect PL of the substrate. However that may be, it is clearly seen that the behavior of the PL intensity of Nd^{3+} ions versus the annealing temperature is manifestly correlated with the one of Si-np. Reminding that the PL measurements were done under nonresonant excitation, this behavior underlines the strong coupling between Si-np and RE ions, and, accordingly, the potential of sensitizing of Si-np. The increase in the PL intensity of Nd^{3+} is partly explained by the increase in the Si-np density and by the decrease in disorder which provides sources of nonradiative de-excitation channels of Si-np and Nd^{3+}. The Nd^{3+} PL intensity is then more efficient after annealing at 1100 °C.

Figure 5 shows the behavior of the PL spectra of the thin films annealed at 1100 °C as a function of the Nd concentration. As the Nd content increases from 0.08 to 0.27 at.%, the PL intensity of Si-np drastically drops and disappears at 1.68 at.%. Then, PL of Si-np surprisingly reappears at the highest Nd concentration of 4.9 at.%. Interestingly, one can observe that the positions and widths of the PL peaks of samples A and B remain identical (see the inset); whereas the PL peak of sample D is manifestly shifted to longer wavelengths. According to the quantum confinement model, the PL of sample D therefore emanates from Si-np that are sensibly larger than the ones present in samples A and B; whereas in the latter samples, a change in the density of luminescent Si-np without any modification of the size distribution is observed. In the infrared spectral domain, one can observe that the PL intensity of Nd^{3+} ions drops with the increase in the Nd concentration.

Figure 6 shows the PL spectra of the most luminescent sample under two excitation wavelengths of 266 and 488 nm. One can observe that the three PL peaks of Nd^{3+} are similar, whereas the spectra significantly change in the visible domain. Indeed, the visible PL peak collected after 488 nm excitation is narrower and shifted to longer wavelengths compared to the counterpart recorded under 266 nm excitation. In order to better understand this behavior, the excitation wavelength dependence of this sample is investigated in the next part of this article using our TPLE system.

C. PL excitation spectroscopy

In Fig. 7(a) is shown the TPLE spectral map of sample A. Again, one can clearly recognize the broad visible PL band and an infrared peak that corresponds to the $^4F_{3/2} \rightarrow {}^4I_{9/2}$ transition of Nd^{3+} ions. In the same manner as in Fig. 6, one can observe that the visible PL band recorded at the longer excitation wavelengths is narrowed and shifted to longer wavelengths compared with the ones obtained at shorter excitation wavelengths. As a consequence, it appears

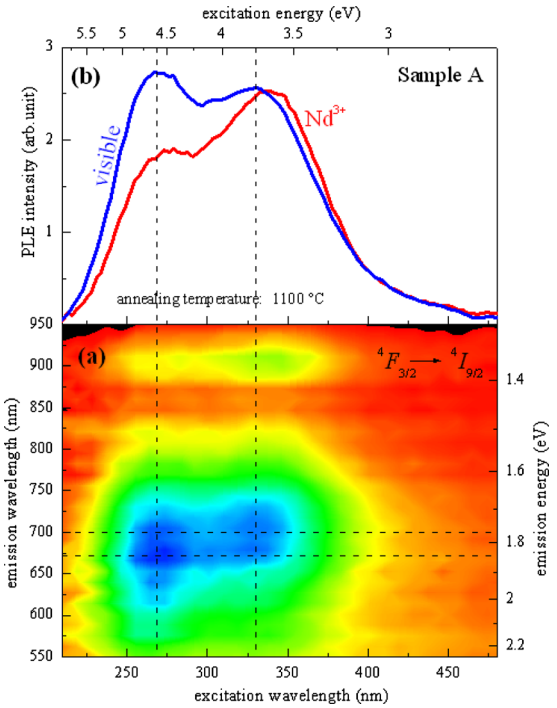

FIG. 7. (Color online) TPLE spectral map of sample A (a) and PL excitation (PLE) spectra of the broad visible band and the PL peak of Nd^{3+} ions (b). The PLE spectra were obtained by integrating the broad visible PL band and the PL peak of Nd^{3+} ions.

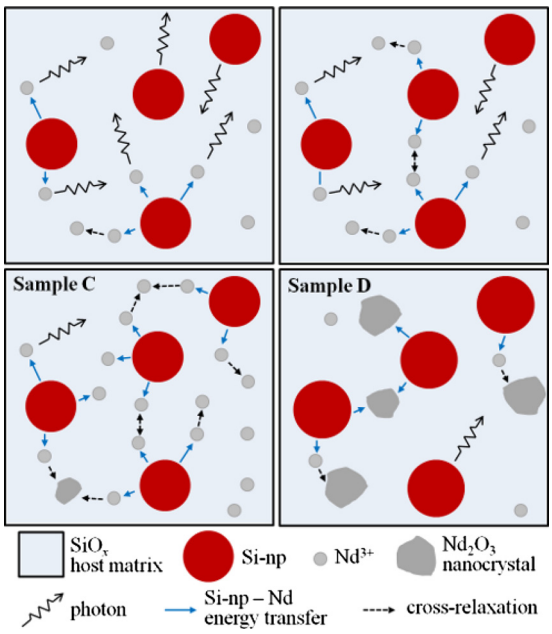

FIG. 8. (Color online) Schematic illustration of a model of the evolution of PL of Si-np Nd^{3+} ions as function of the Nd concentration.

that photons with energies above 4.1 eV are able to excite luminescent species that exhibit light between 600 and 650 nm. In this spectral domain, PL may emanate from residual defect luminescence species in silicates and/or from small Si-np. While photons have excitation energies below 4.1 eV, the PL is mainly originating from excitons confined in Si-np. One can then recognize two maxima at 4.6 and 3.75 eV in the PLE spectrum of the visible PL band [Fig. 7(b)]. The first one may originate from defect PL, as shown by several researchers who studied defects PL (non-bridging oxygen hole centers) in silicates,[33,34] and/or from small Si-np as obtained from simulations elsewhere,[35] while the second one is attributed to the recombination of excitonic states in Si-np, as established by many groups.[17,36–38]

No resonant PL peak of Nd^{3+} was observed in this spectral range, as reported elsewhere.[17] Therefore, no Nd absorption occurs with the excitation power densities that were used. A comparison of the PLE spectra of the visible emission and the infrared peak is shown in Fig. 7(b). It is observed that the shapes of the PLE spectra are similar demonstrating that the excitation process of Nd^{3+} ions is manifestly connected to the luminescent visible species. It is clearly seen that Si-np are the most efficient sensitizers of the PL of Nd^{3+} ions, since the maximum of the PLE spectrum of Nd^{3+} coincides with the one of Si-np. The presence of a weak 270 nm shoulder in the PLE spectrum of Nd^{3+} ions indicates that defects states and/or small Si-np play also the same role but to a lesser extent.

IV. DISCUSSIONS

During the annealing, a phase separation occurs leading to the formation of Si-np as shown in the FTIR spectra in Fig. 1. In the same time, it is shown that disorder, which is a potential source of nonradiative channels, decreases in the host silicate matrix. The incorporation of Nd results in the increase in disorder as shown in Fig. 2. As a consequence, the decrease in the PL of Si-np with increasing Nd content (Fig. 5) is explained by the raise of energy transfer between Si-np and Nd^{3+} ions (which can be luminescent or not), and by the increase in nonradiative recombinations. The Si-np PL quenching due to defects within the Si-np volume induced by the Nd incorporation may be excluded since the solubility of RE in crystalline or amorphous Si is rather low in comparison with silica.[3] Moreover, Fig. 3 shows that Nd_2O_3 nanocrystals are formed at a Nd concentration of 4.9 at.% (sample D). The occurrence of such phase in sample D is supported by the progressive increase in the refractive index while the Nd concentration was increased (Fig. 2). The presence of a Nd_2O_3 phase in the host matrix significantly modifies the number of oxygen atoms available to form the silicon oxide host matrix consequently leading to the formation of larger Si-np with a higher density. Besides, (see Fig. 8) the formation of Nd_2O_3 nanocrystals results in the raise of the average interaction distance between Si-np and Nd atoms (agglomerated or not) leading to the occurrence of not-coupled Si-np therefore enable to emit light. This explains the presence of the PL peak of Si-np in sample D (Fig. 5) which is significantly shifted to longer wavelengths. According to the quantum confinement model, longer emission wavelengths are characteristic of larger Si-np. The fact that x-ray pattern of Si nanocrystals were detected in sample D and not in sample A (Fig. 3) may be also due to the modification of the Si-np density.

The concentration quenching of the PL of Nd^{3+} ions (see Fig. 5) is partly explained by cross relaxation processes between Nd^{3+} ions and neighboring Nd^{3+} ions or Nd_2O_3 nanocrystals (Fig. 8) as reported in glass matrices.[39,40] This is supported by the existence of Nd_2O_3 nanocrystals in the

highest Nd-doped sample. Besides, nonradiative channels inherent to disorder induced by the Nd incorporation (Fig. 2) can be in competition with the energy transfer mechanism between Si-np and Nd^{3+} ions in such nanocomposite systems leading to the common decrease in the PL intensity of Nd^{3+} and Si-np, which is in fact observed (Fig. 5). As a consequence, the emission of Nd^{3+} ions is more efficient while Si-np are formed, and while the Nd content is low (0.08 at.%). In such conditions, Nd^{3+} ions benefit from the sensitizing effect of Si-np and from the weak competition of nonradiative recombinations in the host matrix and concentration quenching processes.

TPLE measurement showed that the excitation spectrum of Nd^{3+} ions is clearly correlated with the excitation mechanism of Si-np, demonstrating the energy transfer from Si-np toward Nd^{3+} ions. The efficiency of the energy transfer is maximal at 340 nm which corresponds to the maximum of radiative deexcitation of Si-np.

V. CONCLUSIONS

We have investigated the microstructure and the PL properties of Nd-doped SRSO thin films having the same Si excess. We showed that the maximum of the PL intensity of Nd^{3+} ions is obtained after annealing at 1100 °C which corresponds to the better situation for the achievement of high luminescent Si-np embedded in SiO_2, i.e., containing a small quantity nonradiative recombination channels. We showed that the PL of Nd^{3+} ions is quenched at high Nd-concentration (4.9 at.%) because of the formation of Nd_2O_3 nanocrystals and the occurrence of disorder in the host matrix. The former participates to the concentration quenching mechanism due to cross relaxation processes, while the latter induced the occurrence of new nonradiative channels which are in competition with the energy transfer mechanism between Si-np and Nd^{3+} ions. Our TPLE measurements show that the excitation energy dependence of Nd^{3+} ions is nonresonant and follows the one of Si-np. This new result unambiguously demonstrates that an energy transfer occurs from Si-np to Nd^{3+} ions.

ACKNOWLEDGMENTS

The authors are grateful to the French-Polish joint project POLONIUM (PHC, EGIDE) for their financial support of our work. G. Zatryb and A. Podhorodecki acknowledge financial support from fellowship co-financed by European Union within European Social Fund. The French team thanks the French Agence Nationale de la Recherche, which supported this work through the Nanoscience and Nanotechnology program (DAPHNES Project No. ANR-08-NANO-005).

[1] E. Desurvire, Phys. Today **47**(1), 20 (1994).
[2] W. F. Krupke, IEEE J. Quantum Electron. **10**, 450 (1974).
[3] A. J. Kenyon, Prog. Quantum Electron. **26**, 225 (2002).
[4] W. J. Miniscalco, J. Lightwave Technol. **9**, 234 (1991).
[5] A. Polman, J. Appl. Phys. **82**, 1 (1997).
[6] J. H. Campbell and T. I. Suratwala, J. Non-Cryst. Solids **263-264**, 318 (2000).
[7] J. Wang, L. Reekie, W. S. Brocklesby, Y. T. Chow, and D. N. Payne, J. Non-Cryst. Solids **180**, 207 (1995).
[8] A. J. Kenyon, P. F. Trwoga, M. Federighi, and C. W. Pitt, J. Phys.: Condens. Matter **6**, L319 (1994).
[9] A. J. Kenyon, C. E. Chryssou, C. W. Pitt, T. Shimizu-Iwayama, D. Hole, N. Sharma, and C. J. Humpreys, J. Appl. Phys. **91**, 367 (2002).
[10] G. Franzò, V. Vinciguerra, and F. Priolo, Appl. Phys. A: Mater. Sci. Process. **69**, 3 (1999).
[11] K. Watanabe, H. Tamaoka, M. Fujii, K. Moriwaki, and S. Hayashi, Physica E **13**, 1038 (2002).
[12] S.-Y. Seo, M.-J. Kim, and J. Shin, Appl. Phys. Lett. **83**, 2778 (2003).
[13] A. N. MacDonald, A. Hryciw, F. Lenz, and A. Meldrum, Appl. Phys. Lett. **89**, 173132 (2006).
[14] D. Bréard, F. Gourbilleau, C. Dufour, R. Rizk, J.-L. Doulan, and P. Camy, Mater. Sci. Eng. **146**, 179 (2008).
[15] D. Bréard, F. Gourbilleau, A. Belarouci, C. Dufour, and R. Rizk, J. Lumin. **121**, 209 (2006).
[16] F. Gourbilleau, A. Belarouci, D. Bréard, C. Dufour, and R. Rizk, Int. J. Nanotechnol. **5**, 574 (2008).
[17] A. Podhorodecki, J. Misiewicz, F. Gourbilleau, J. Cardin, and C. Dufour, Electrochem. Solid-State Lett. **13**, K26 (2010).
[18] C. Ternon, F. Gourbilleau, X. Portier, P. Voivenel, and C. Dufour, Thin Solid Films **419**, 5 (2002).
[19] S. Charvet, R. Madelon, F. Gourbilleau, and R. Rizk, J. Appl. Phys. **85**, 4032 (1999).
[20] B. J. Hinds, F. Wang, D. M. Wolfe, C. L. Hinkle, and G. Lucovsky, J. Non-Cryst. Solids **227–230**, 507 (1998).
[21] H. Ono, T. Ikarashi, K. Ando, and T. Kitano, J. Appl. Phys. **84**, 6064 (1998).
[22] F. Gourbilleau, C. Dufour, M. Levalois, J. Vicens, R. Rizk, C. Sada, F. Enrichi, and G. Battaglin, J. Appl. Phys. **94**, 3869 (2003).
[23] A. Fidalgo and L. M. Ilharco, J. Non-Cryst. Solids **283**, 144 (2001).
[24] P. Innocenzi, J. Non-Cryst. Solids **316**, 309 (2003).
[25] H. Ono and T. Katsumata, Appl. Phys. Lett. **78**, 1832 (2001).
[26] O. Medenbach, D. Dettmar, R. D. Shannon, R. X. Fischer, and W. M. Yen, J. Opt. A, Pure Appl. Opt. **3**, 174 (2001).
[27] V. Kapaklis, J. Non-Cryst. Solids **354**, 612 (2008).
[28] L. Kępiński, M. Zawadzki, and W. Miśta, Solid State Sci. **6**, 1327 (2004).
[29] B. Lal, S. Kumar, P. Aghamkar, S. Rohilla, and D. Singh, Physica B **404**, 3452 (2009).
[30] B. Garrido, M. Lòpez, A. Pérez-Rodríguez, C. García, P. Pellegrino, R. Ferré, J. A. Moreno, J. R. Morante, C. Bonafos, M. Carrada, A. Claverie, J. de la Torre, and A. Souifi, Nucl. Instrum. Methods Phys. Res. B **216**, 213 (2004).
[31] V. V. Bolotov and V. E. Kan, Physica B **404**, 4555 (2009).
[32] R. K. Ahrenkiel, S. W. Johnston, W. K. Metzger, and P. Dippo, J. Electron. Mater. **37**, 396 (2008).
[33] M. Cannas, L. Vaccaro, and B. Boizot, J. Non-Cryst. Solids **352**, 203 (2006).
[34] L. Skuja, J. Non-Cryst. Solids **239**, 16 (1998).
[35] C. Bulutay, Phys. Rev. B **76**, 205321 (2007).
[36] A. Podhorodecki, J. Misiewicz, F. Gourbilleau, and R. Rizk, Electrochem. Solid-State Lett. **11**, K31 (2008).
[37] Y. H. Xie, W. L. Wilson, F. M. Ross, J. A. Mucha, E. A. Fitzgerald, J. M. Macaulay, and T. D. Harris, J. Appl. Phys. **71**, 2403 (1992).
[38] S. Sinha, S. Banejee, and M. Arora, Phys. Rev. B **49**, 5706 (1994).
[39] J. A. Caird, A. J. Ramponi, and P. R. Staver, JOSA B **8**, 1391 (1991).
[40] C. Jacinto, S. L. Oliveira, L. A. O. Nunes, M. J. Myers, and T. Catunda, Phys. Rev. B **73**, 125107 (2006).